Hindawi
Journal of Nanomaterials
Volume 2022, Article ID 2453412, 15 pages
https://doi.org/10.1155/2022/2453412

Research Article

Optimization and Mechanical Characteristics of AA6061/Zirconia Nanocomposites Fabricated by Ultrasonic-Aided Stir Casting Method

Amel Gacem,[1] Moamen S. Refat,[2] H. Elhosiny Ali,[3,4,5] S. C. V. Ramana Murty Naidu,[6] B. Beenarani,[7] Pranjali Deole,[8] S. Sandeep Kumar,[9] S. Rama,[10] Amnah Mohammed Alsuhaibani,[11] and Abdi Diriba[12]

[1]*Department of Physics, Faculty of Sciences, University 20 Août 1955, 26 El Hadaiek, Skikda 21000, Algeria*
[2]*Department of Chemistry, College of Science, Taif University, P.O. Box 11099, Taif 21944, Saudi Arabia*
[3]*Research Center for Advanced Materials Science (RCAMS), King Khalid University, Abha 61413, P.O. Box 9004, Saudi Arabia*
[4]*Department of Physics, Faculty of Science, King Khalid University, Abha 61413, Saudi Arabia*
[5]*Department of Physics, Faculty of Science, Zagazig University, Zagazig, Egypt*
[6]*Department of Mechanical Engineering, Sri Venkateswara College of Engineering & Technology, Etcherla, Srikakulam, Andhra Pradesh 532410, India*
[7]*Department of Computer Science Engineering, Saveetha School of Engineering, SIMATS, Chennai, Tamil Nadu 600124, India*
[8]*Department of Mechanical Engineering, Shri Ramdeobaba College of Engineering and Management, Nagpur, Maharashtra 440013, India*
[9]*Department of Computer Science Engineering, Koneru Lakshmaiah Education Foundation, Vaddeswaram, Andhra Pradesh 522302, India*
[10]*Department of Mechanical Engineering, Gokaraju Rangaraju Institute of Engineering and Technology, Hyderabad, Telangana 500090, India*
[11]*Department of Physical Sport Science, College of Education, Princess Nourah bint Abdulrahman University, P.O. Box 84428, Riyadh 11671, Saudi Arabia*
[12]*Department of Mechanical Engineering, Mizan Tepi University, Ethiopia*

Correspondence should be addressed to Abdi Diriba; abdi@mtu.edu.et

Received 8 May 2022; Revised 16 July 2022; Accepted 19 July 2022; Published 20 September 2022

Academic Editor: Arpita Roy

Using the Taguchi Grey response surface approach, this study investigates the effect of novel ultrasonic-aided stir casting conditions on the production of AA6061/zirconia nanocomposites. A Taguchi L_{16} orthogonal array was utilized to conduct the researches, which included ultrasonic power (1.75-2.5 kW), time (5-20 min), temperature (750-900°C), which can cause premature solidification, stir pressure (100-250 MPa), and reinforcement weight percentage (wt% of reinforcement). Ultrasonic-aided stir casting technique has five adjustable parameters (2-5). The ultimate tensile strength, elongation percentage, hardness, and size of the grain material were some of the metrics used to evaluate the process performance. It was decided to employ the response surface approach to model and optimize the numerous replies into one grey relational analysis. AA6061/zirconia nanocomposites were studied using statistical methods such as 3D surface plots and variance analysis. 2.2537 kW, 16.28 min ultrasonic duration, weight % of reinforcement of 1.9, stirring temperature of 700.73°C, and stirring pressure of 142.63 MPa were found to be the best parameter values.

1. Introduction

In a variety of industries, metal matrix composites play an important role due to their light weight, greater durability, and outstanding resistance to wear as well as corrosion [1]. Lightweight aluminum matrix composites (AMCs) are employed in several technical applications because they have tensile strength, less coefficient of thermal expansion [2], increased mechanical and anticorrosion qualities, and a less coefficient of thermal extension [3, 4]. In contrast, the mechanical characteristics of aluminum matrix composites are strongly reliant on the kind, quantity, and nature of the strengthening properties contained in its matrix [5]. AA6061 is a heating-resistant metal of aluminum and Cu that is a common alloying element [6]. Weight, strength, and corrosion resistance (and high machinability) make them ideal for use in aerospace or automobile engineering. A chemically inert ceramic with outstanding thermomechanical characteristics, zirconia (ZrO_2) is a versatile material [7]. For example, zirconia's density is 3.95 grams per cubic centimeter, its melting point is 2056°C, and its thermal expansion coefficient is 7.4 μm/°C. Zirconia reinforcements have been found to greatly upgrade the mechanical characteristics of aluminum alloys in previous studies [8, 9]. Furthermore, nanosized zirconia elements have a significant impact on the mechanics and thermomechanic characteristics of nanostructured owing to their high surface-to-volume proportion [10]. MMCs with near net forms can be produced using the liquid metallurgical process known as stir casting [11]. Since it eliminates porosity and improves surface texture and mechanical qualities while also utilizing a finer microstructure than conventional casting, stir casting is a preferable method [12]. While traditional stir casting may be used to introduce nanoparticles [13] into the metal matrix, it is quite difficult to do so. Excessive churning will result in the matrix being oxidized and clumping together [14]. In these circumstances, ultrasonic therapy (UST) can be employed to efficiently distribute nanosized reinforcements [15]. Grains are refined and degassed using UST in the composite production sectors. When high-intensity ultrasonic waves are used during ultrasonic therapy, the melt is subjected to intense cavitation and acoustic streaming. Because of this, ultrasonic therapy breaks apart nanoparticulate groups and evenly disperses the particles that make up the material melt [16]. It is therefore ineffective to just employ the use of ultrasonic therapy in the production of nanocomposites. To improve nanocomposites' microstructure and mechanical characteristics, the ultrasonic therapy stir casting process is a common production technique [17]. Many recent studies have shown that adjusting the casting process parameters utilizing various optimization tools may improve the mechanical and microstructural characteristics of composites [18]. It was found that 106 MPa, 200°C, and 30 s are the optimal values for stir casting pressure, die heating temperature, and stir duration for the stir casting method of LM_{24} alloy to increase the UTS and stiffness. Wetting of dispersion issues was resolved by treating AA6061/1 wt% ZrO_2 nanocomposites with ultrasonic treatment, which caused in a rise in ultimate tensile strength yield of 37% and 81%, correspondingly, as equated to the base alloy [19]. It was found that ultrasonic processing with a 1400 W/cm^{-2} power level and a 5% solute concentration resulted in the best grain refinement in a study by [20]. With the help of T-GRA and ANOVA, [21] investigated whether process parameters (UTS, stiffness, and % of extension) affected the microstructure and mechanical characteristics of AA6061-ZrO_2 compounds (ANOVA). The optimal values were discovered to be a stirring pressure of 128 MPa, a molten temperature of 848°C, and a weight percentage of SiC [22]. Improve multiple responses processes with the use of the RSM and examination of the desirability approach, two commonly used methodologies. It is possible to determine the best input conditions using these methods. An ANOVA, RSM, and a desirability function-based technique was utilized by [23] to identify the best combinations of manufacturing parameter A413 alloy, which is made by stir casting. It was found that the physical and microstructural characteristics of LM_{13} alloy were affected by molten metal and die temperatures, as well as stir pressure. Higher stir pressure decreased grain size and enhanced hardness and density, according to the data [24]. However, hardness declined with increasing melt and die temperatures. Microstructure and mechanical characteristics of 6061 alloy AA were examined by [25]. Assuming 700°C and 140 MPa, the average grain size was 80 nm. Pouring temperature had no effect when the stir pressure was more than 70 MPa. To improve the wear characteristics of AA7150-hBN composites, [26] utilize Taguchi L_{25} orthogonal array-ANOVA. Taguchi's L_{16} orthogonal array, stirring pressure, pressure holding duration, and die preheating temperature all had a significant impact on composite reactions including stiffness and high strengthening, according to [27, 28] employing an artificial neural network prediction model to investigate how the settings used in stir casting affected the solidification time. It was shown that both the mold and pouring temperatures had significant effects on casting quality and freeze time. For AA2024-SiC nanocomposites, [29] established remarkably low error % artificial neural network models to forecast the density and hardness. Stir casting processing parameters include pouring temperature, pressuring duration, and die temperature which were examined in depth by [30]. Nanocomposites using traditional stir-stir casting have had difficulty achieving acceptable microstructural and mechanical qualities, as has been widely documented in previous investigations [31]. These obstacles can be

Table 1: Characteristics of zirconia.

Property	Values
Density	6.15 g/cm^3
Colour	White
Melting point	2973 K
Shape	Spherical

Table 2: Processing factors and its levels.

Processing factors	Level 1	Level 2	Level 3	Level 4
Ultrasonic therapy power (KW) (A)	1.75	2	2.25	2.5
UST time (min) (B)	5	10	15	20
Pouring temperature (°C) (C)	750	800	850	900
Squeezing pressure (MPa) (D)	100	150	200	250
Weight percentage of reinforcement (wt%) (E)	2	3	4	5

solved by employing a technology known as ultrasonication-stir linked stir casting, which has proven effective in the last several years. No one has employed an optimal combination of ultrasonic therapy stir casting parameters, and the literature study clearly shows that there is a considerable need for improving these parameters to fabricate aluminum nanocomposites. According to [32], L_{16} orthogonal array 16 distinct AA6061/zirconia nanocomposites were made utilizing the UST-stir linked stir casting process. There were five variables that could be tweaked in the ultrasonic-aided stir casting process: power (1.75-2.5 kW), duration (5-20 min), pour temperature (750-900°C), stir pressure (100-250 MPa), and wt% ZrO_2 (2-5%). The results were analyzed using these parameters. We selected hardness, elongation percentage, and particle size as the replies. The TGRSM approach was utilized to invent the finest mixture of parameters [33–35]. The best condition was verified by conducting a desire analysis and a confirmation experiment.

2. Methods and Materials

2.1. Matrix and Reinforcement. It was decided to use zirconia alloy 6061 as the matrix composite in this study. The nanopowder of zirconia (ZrO_2) was used as reinforcement. Table 1 lists the characteristics of ZrO_2.

2.2. Selection of Process Parameters and Responses. For high-quality castings, it is vital to pick the right casting process parameters and operating levels. Selecting control parameters with an inadequately big or narrow operating range, you may end up with a flawed or incomplete solution. Nanoparticle aggregation and matrix material oxidation would occur if the ultrasonic therapy power and the ultrasonic therapy duration were increased [34]. Lower ultrasonic therapy power and duration, on the other hand, are insufficient for dissolving nanoparticle clusters and removing dendrites from microstructures. Due to a delayed cooling rate, dendritic structures emerge when the melt is poured at a higher temperature. Premature solidification might occur if the pouring temperature is too low and the processing parameters are shown in Table 2.

2.3. AA6061/Zirconia Nanocomposite Fabrication. Initial melting was done in mild steel employing an electric resistance furnace with highest heating system of 1200°C. A K-type thermocouple has been used to show the temperature of the furnace and the melt. We used an inert gas shield to safeguard the melting process. Zirconia nanoparticles were also dried in a muffle furnace by heating them to 300°C for an hour. The composites were manually stirred for two minutes at 500 revolutions per minute utilizing a graphene layered stainless steel stirrer when it reached the appropriate melting temperature. Zirconia nanopowder was added to the melt and agitated for another 5 minutes before being removed [35]. A titanium alloy ultrasonic probe was used to disseminate ultrasonic waves into the slurry after adequate churning. The sonotrode was submerged in the melting space to a deepness of 300 mm during the ultrasonication operation. Power was raised to 2.5 kilowatt and the frequency was set at 20 kHz. Warm steel mold dies (300 mm high by 50 mm wide) were used to bottom-pour the melt before it could harden. It was critical that all of the experiments be conducted with a 1-minute stir period. Accordingly, the process parameters for producing the 16 distinct AA6061/zirconia nanocomposites were adjusted according to the Taguchi L_{16} orthogonal array. A high-precision weighing scale (accurate to 0.00001 g) was used to measure the porosity of the manufactured materials.

2.4. Heat Treatment of Nanocomposites. Precipitation hardening under a T-6 tempering condition hardened the nanocomposites. In solution treatment, the nanocomposites were maintained at 510°C for two hours before being immediately quenched in water. In addition, the aging process was carried out for 14 hours at 165°C. Heat treatment was done in an argon endangered atmosphere employing a high-temperature muffle boiler. In a double disc-polishing machine, abrasive polishing sheets of 400, 600, 1200, and 2000 grit were used to make microstructural study specimens. Particle size was determined using the ASTM E 112-96 linear intercept method.

2.5. Hardness Test. Nanocomposites were tested for microhardness (VHN) using a Vickers hardness tester (Bluestar Vickers hardness tester). Indentation testing was performed on the polished specimens using a 10 kg load as well as a dwell duration of 15 seconds.

2.6. Tensile Test. Tensile tests were conducted to determine how casting factors affected the nanocomposites' ultimate tensile strength and elongation %. Figure 1 indicates the specimen schematic of tensile tests done on an Instron tensile testing equipment with a strain rate of 1 mm/min. A gauge span of 251 mm was used for the tensile test, which

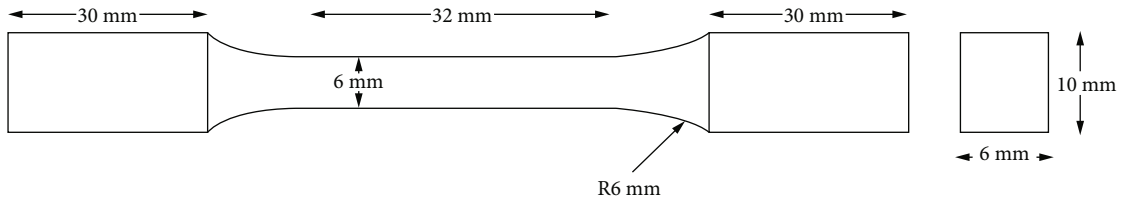

Figure 1: Measurement of the tensile test sample.

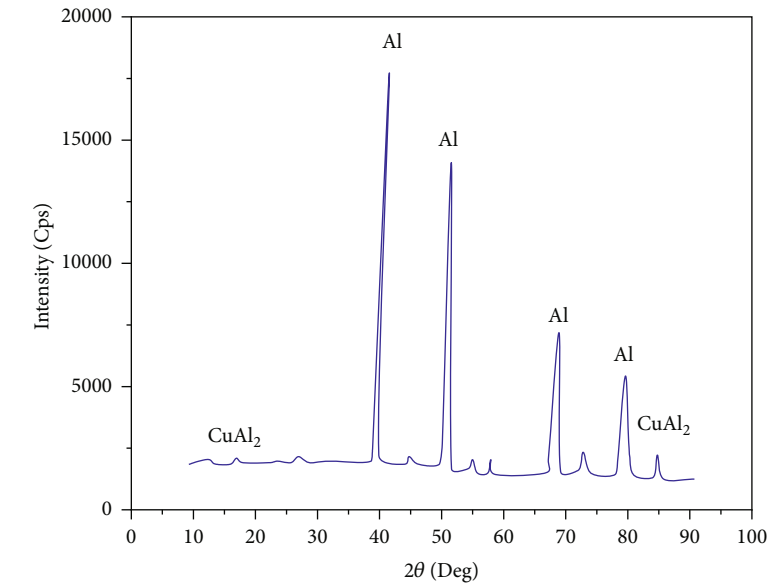

(a)

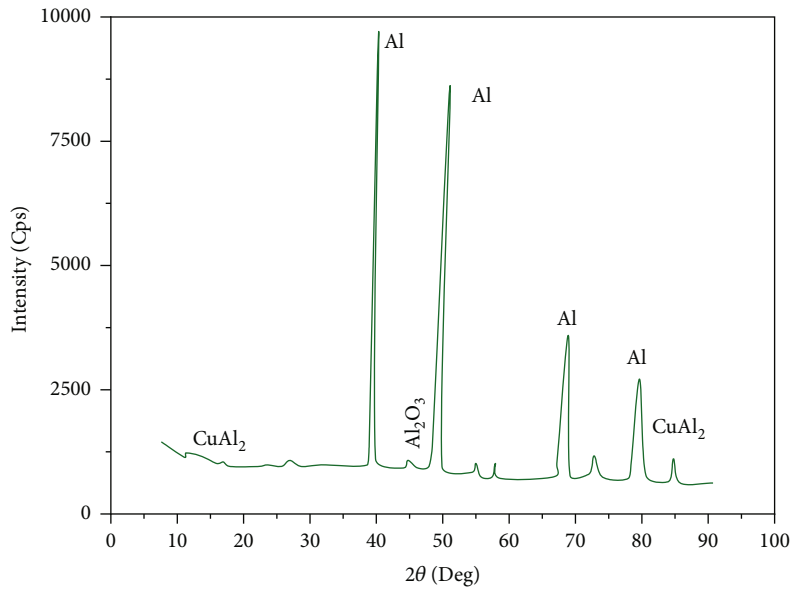

(b)

Figure 2: XRD forms of materials: (a) AA6061 and (b) zirconia.

Table 3: Orthogonal arrangement and experimental outcome on Taguchi L_{16}.

Exp. no.	Processing factors					Hardness (VHN)		Ultimate tensile strength (MPa)		Elongation (%)		Grain size	
	A (watt)	B (min)	C (°C)	D (MPa)	E (wt%)	R1	R2	R1	R2	R1	R2	R1	R2
1	1750	5	750	100	2	124	124	245	226	6.4	6.3	197	197
2	1750	10	800	150	3	126	127	247	268	4.7	6.8	176	174
3	1750	15	850	200	4	127	125	278	274	3.7	6.0	162	166
4	1750	20	900	250	5	122	116	228	234	4.1	3.1	222	208
5	2000	5	800	100	2	128	135	257	274	4.9	4.9	180	176
6	2000	10	850	150	3	137	136	311	291	6.9	6.5	147	139
7	2000	15	900	200	4	134	134	294	304	7.2	6.9	149	150
8	2000	20	750	250	5	128	126	296	272	8.1	10.3	165	169
9	2250	5	800	150	2	138	144	302	331	7.5	7.9	125	127
10	2250	10	850	100	3	132	129	297	301	9.9	9.0	146	142
11	2250	15	900	250	4	144	142	291	305	6.9	6.7	126	128
12	2250	20	750	200	5	138	137	321	314	6.8	7.5	130	130
13	2500	5	850	100	3	146	141	321	334	7.1	9.1	90	90
14	2500	10	800	150	4	140	139	301	273	7.2	7.4	116	112
15	2500	15	900	200	2	143	137	312	337	10.5	11.9	70	64
16	2500	20	750	250	5	149	149	336	340	10.6	10.7	45	41

Table 4: Normalized and sound to noise ratio values of trials.

Exp. no.	Sound to noise ratio values				Normalized sound to noise ratio values			
	Hardness (VHN)	Ultimate tensile strength (MPa)	Elongation (%)	Grain size (μm)	Hardness (VHN)	Ultimate tensile strength (MPa)	Elongation (%)	Grain size (μm)
1	42.869	48.409	16.056	45.892	0.188	0.042	0.53	0.946
2	42.043	48.195	15.757	44.872	0.276	0.279	0.394	0.873
3	42.008	48.828	13.976	45.378	0.256	0.472	0.209	0.832
4	42.504	48.278	10.875	46.645	0.000	0.000	0.000	1.000
5	42.368	48.455	13.803	-45.009	0.443	0.357	0.296	0.882
6	42.703	49.556	16.512	-43.110	0.613	0.690	0.564	0.746
7	42.543	49.502	16.954	43.493	0.514	0.674	0.613	0.774
8	42.077	49.043	19.088	44.455	0.293	0.535	0.818	0.843
9	42.979	49.974	17.723	42.008	0.754	0.817	0.686	0.668
10	42.311	49.513	19.478	43.168	0.413	0.677	0.855	0.751
11	43.107	49.477	16.646	42.076	0.819	0.666	0.578	0.672
12	42.768	50.028	17.056	42.279	0.645	0.833	0.623	0.687
13	43.134	50.298	17.972	39.085	0.832	0.915	0.712	0.458
14	42.892	49.127	17.265	41.139	0.709	0.560	0.642	0.605
15	42.913	50.212	20.934	36.530	0.723	0.889	1.000	0.276
16	43.465	50.578	20.548	32.679	1.000	1.000	0.97	0

Table 5: GRC and grey relational grade values.

Exp. no.	GRC				Grey relational grade	Rank
	Hardness (VHN)	Elongation (%)	Grain size (μm)	Ultimate tensile strength (MPa)		
1	0.382	0.511	0.902	0.343	0.5337	12
2	0.409	0.453	0.797	0.408	0.5163	14
3	0.403	0.388	0.749	0.486	0.5058	15
4	0.334	0.334	1.000	0.334	0.5000	16
5	0.474	0.416	0.808	0.438	0.5337	13
6	0.564	0.535	0.665	0.618	0.5945	9
7	0.516	0.564	0.688	0.606	0.5933	10
8	0.415	0.733	0.762	0.512	0.6064	8
9	0.668	0.614	0.602	0.733	0.6539	4
10	0.461	0.775	0.668	0.609	0.6272	6
11	0.734	0.543	0.605	0.601	0.6197	7
12	0.585	0.568	0.616	0.751	0.6295	5
13	0.748	0.635	0.481	0.856	0.6792	3
14	0.631	0.583	0.558	0.533	0.5761	11
15	0.642	1.000	0.407	0.819	0.7172	2
16	1.000	0.926	0.334	1.000	0.8148	1

was completed successfully. Hardness and tensile testing were performed on samples.

3. Results and Discussion

3.1. Intermetallic Phase Analysis of Nanocomposites. The XRD patterns of AA6061 and AA6061/2 weight % Zr nanocomposite are shown in Figures 2(a) and 2(b), correspondingly. It can be shown in Figure 2(a) that the natural intermetallic phase generated by Cu and Al atoms reacting in the 6061-aluminum alloy corresponds to the peaks associated with both the phase and the intermetallic CuA_{l2} phase. It may be seen in Figure 2(b).

3.2. Process Optimization Using TGRSM. Taguchi L_{16} orthogonal array was employed to done the testing, with two replications for each trial. Results for each stage of the experiment are summarized in Tables 3 and 4. First, the response values were functional to Grey relational analysis and its GRA output was employed as an input for response surface methodology displaying and optimizing. Every set of normalized sound to noise ratio values of replies is used to determine the GRC values. Grey relational grade was created by averaging the GRC values of different GRCs into a single quality index. All responses and their accompanying grey relational grade are shown in Table 5. When grey relational grade reaches its maximum value on the sixteenth trial, it is close to the optimal parameter level. Variations in grey relational grade values, as seen in Figure 3, illustrate that parameter levels selected have a significant influence on the grey relational grade. RSM was used to analyze the grey relational grade values obtained by RSM. Minitab software was used to determine the model coefficients for the second-order polynomial equation that expresses the impact of factors on grey relational grade.

3.3. ANOVA on Grey Relational Grade. The ANOVA was chosen to investigate the most critical factors that contribute to the generation of grey relational grade values. Table 6 indicates the ANOVA outcomes for grey relational grade. While the "*p* value" showed the importance of the model terms, the "*F* value" showed the model's significance. We identified all of the factors and interactions that were examined in the model (A/B/C/D/E) as the most important variables. Table 7 shows that the polynomial model's *R*-squared value was quite near to unity. Using this data, the model is able to forecast future results based on the results of actual experiments.

Figure 4(a) demonstrates the model's suitability. Polynomial model predictions of grey relational grade agree with those obtained under experimental circumstances; it is discovered. The adjusted *R*-squared value was quite close to the projected *R*-squared value. To put this into perspective, the model has an adequate precision of 30.016, as indicated in the tables. Figure 4(b) displays that the studentized residuals follow the normal distribution, as may be demonstrated. This suggests that polynomial models can be used to predict GRG values in the experimental area with reasonable accuracy and precision.

3.4. Grey Relational Grade Surface Plots in 3D. 3D surface plots, as illustrated in Figures 5(a)–5(c), were produced to study the effects of processing factors on grey relational grade. The grey relational grade value is strongly influenced by the ultrasonic therapy power and pouring temperature, as illustrated in Figure 5(a). It has been found that grey relational grade values increase when ultrasonic therapy power

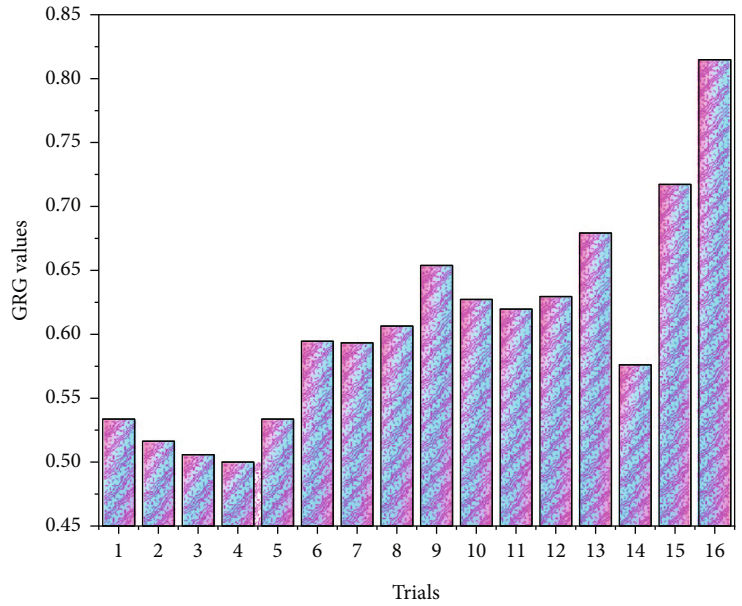

Figure 3: Variations in GRG levels among different trials.

Table 6: ANOVA on grey relational grade.

Source	SS	DoF	Mean square	F value	p value
Model	0.1047	8	0.0133	75.23	<0.0002
A	0.01938	1	0.01947	12.32	0.002
B	0.04415	1	0.04415	26.71	0.002
C	0.00222	1	0.00213	13.35	0.011
D	0.00520	1	0.00511	30.76	0.002
E	0.01179	1	0.01179	69.61	0.000
AC	0.00123	1	0.00123	8.14	0.033
BC	0.00446	1	0.00446	26.92	0.002
DE	0.00665	1	0.00665	39.68	0.000
Residual	0.00121	7	0.000182	—	—
Cor. total	0.105	15	—	—	—

Table 7: Adequate precision values and model adequacy R-squared.

Standard variance	0.0132	R-squared	0.9887
Mean	0.6064	Adjustable R-squared	0.9757
Coefficient of difference	2.1618	Forecast R-squared	0.9049
Forecast residual error SS	0.0064	Adequacy precision	30.0166

increases. Respondent values increased as ultrasonic therapy power increased owing to particle dispersal, grain enhancement, and varied nucleation. Pouring temperatures increase the grey relational grade value. Because the freezing period was prolonged and the number of secondary dendrites increased, there were more secondary dendrite forms. At lower ultrasonic therapy power levels, pouring temperature had little effect. UST time, melt pouring temperature, and other variables, including ultrasonic therapy power (2250 watts), stir pressure (200 MPa), and weight % of reinforcement, are depicted in Figure 5(b) as a function of grey relational grade. The grey relational grade value rises to 0.678 at minimum pouring temperatures and lengthier ultrasonic therapy intervals. Figure 5(b) displays a strong link among the ultrasonic therapy time as well as the pouring temperature. The grey relational grade value fell as the pouring temperature was increased to 900°C. It was found that the grey relational grade was highest when the ultrasonic therapy

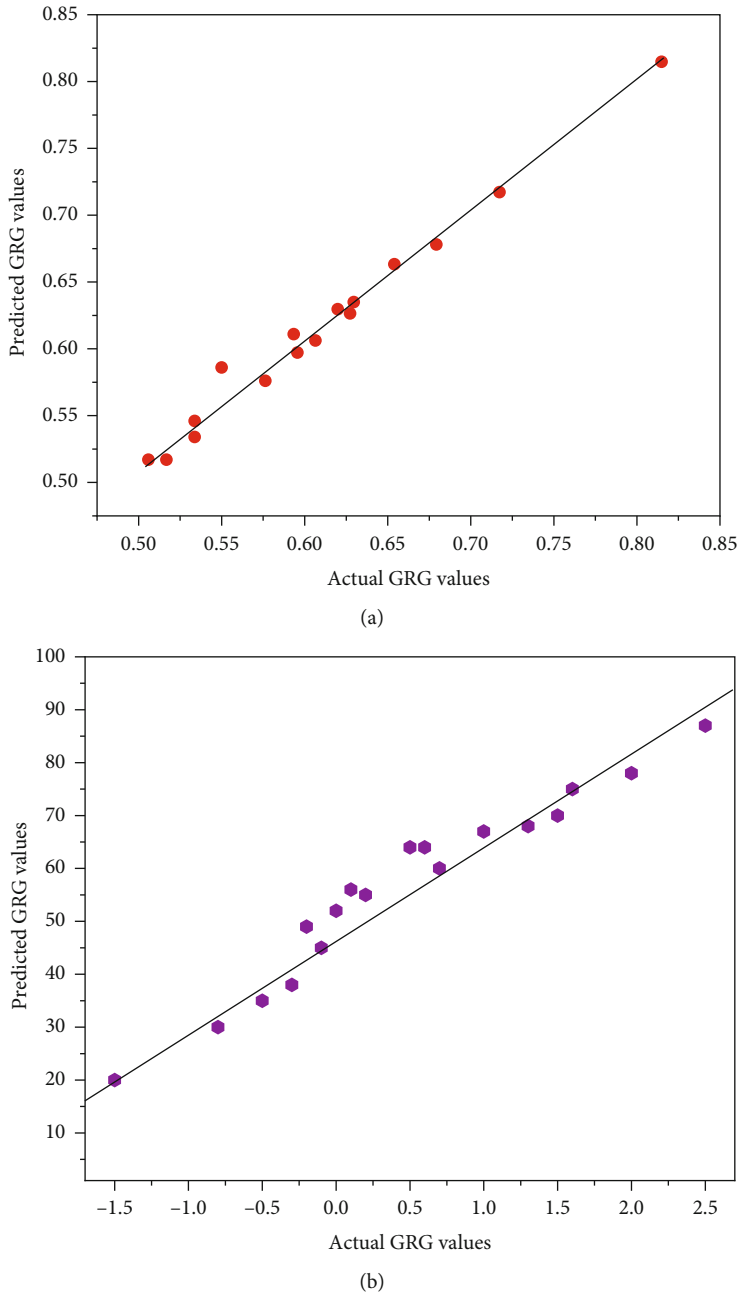

Figure 4: (a) Actual vs. predicted grey relation grade. (b) Studentized residuals vs. normal % probability.

was longer and the pouring temperature was lower. The best strategy to ensure that the product is safe to consume is to increase the ultrasonic therapy duration and lower the pouring temperature as much as feasible. A longer ultrasonic therapy time will reduce the chance of nanoparticle agglomeration. Pouring at a lower temperature speeds up the cooling process, which improves the qualities of the finished product.

Figure 5(c) shows the interaction between stirring pressure and weight percentage. When the ultrasonic therapy power, the ultrasonic therapy duration, and the temperature are all persistent, the grey relational grade values are projected over the assortment of stir pressure and particles weight. According to this diagram, a high grey relational grade is produced when the wt% of particles is 6% and the stirring pressure is 250 MPa. Grain refining, elimination of porosity melt, and dendritic fragmentation all contribute to a rise in the grey relational grade value as the stir pressure increases. At first, an increase in nanoparticle weight % increased the multiperformance of AA6061/zirconia nanocomposites cast by ultrasonic-aided stir casting. Reinforcement with a higher wt% results in an increased grey relational grade; this indicates, therefore, an ideal 3 wt% ZrO_2 concentration for enhanced mechanical properties.

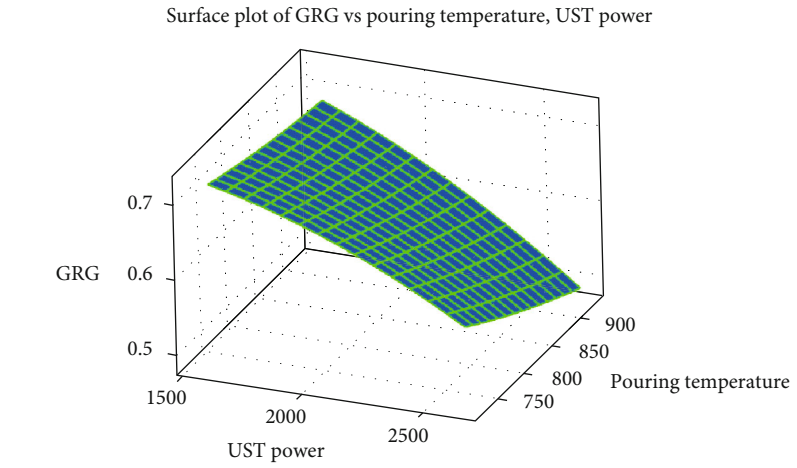

(a)

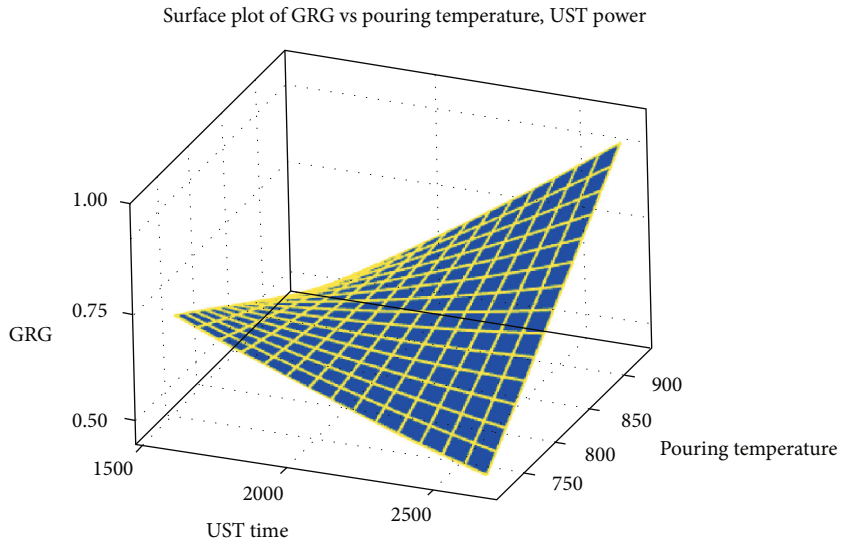

(b)

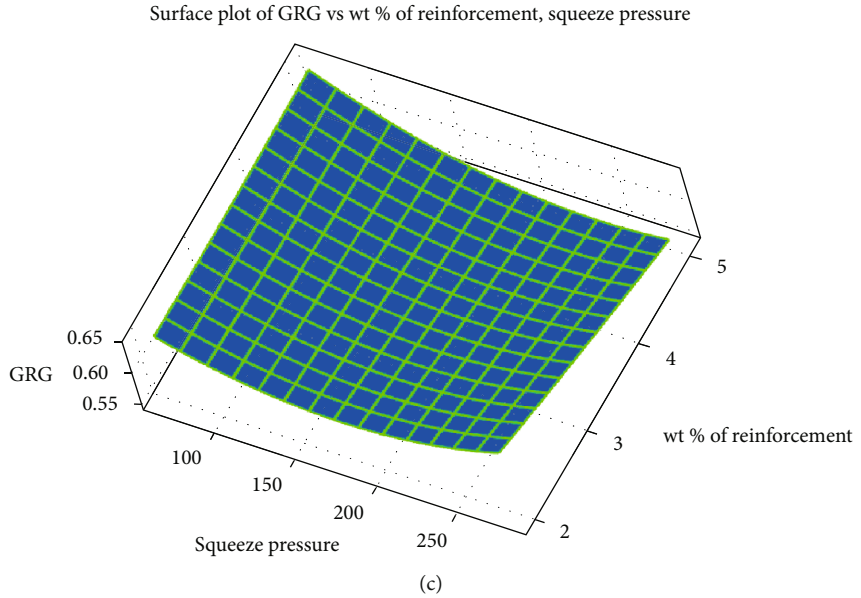

(c)

Figure 5: (a–c) 3D response surface plots of grey relational grade.

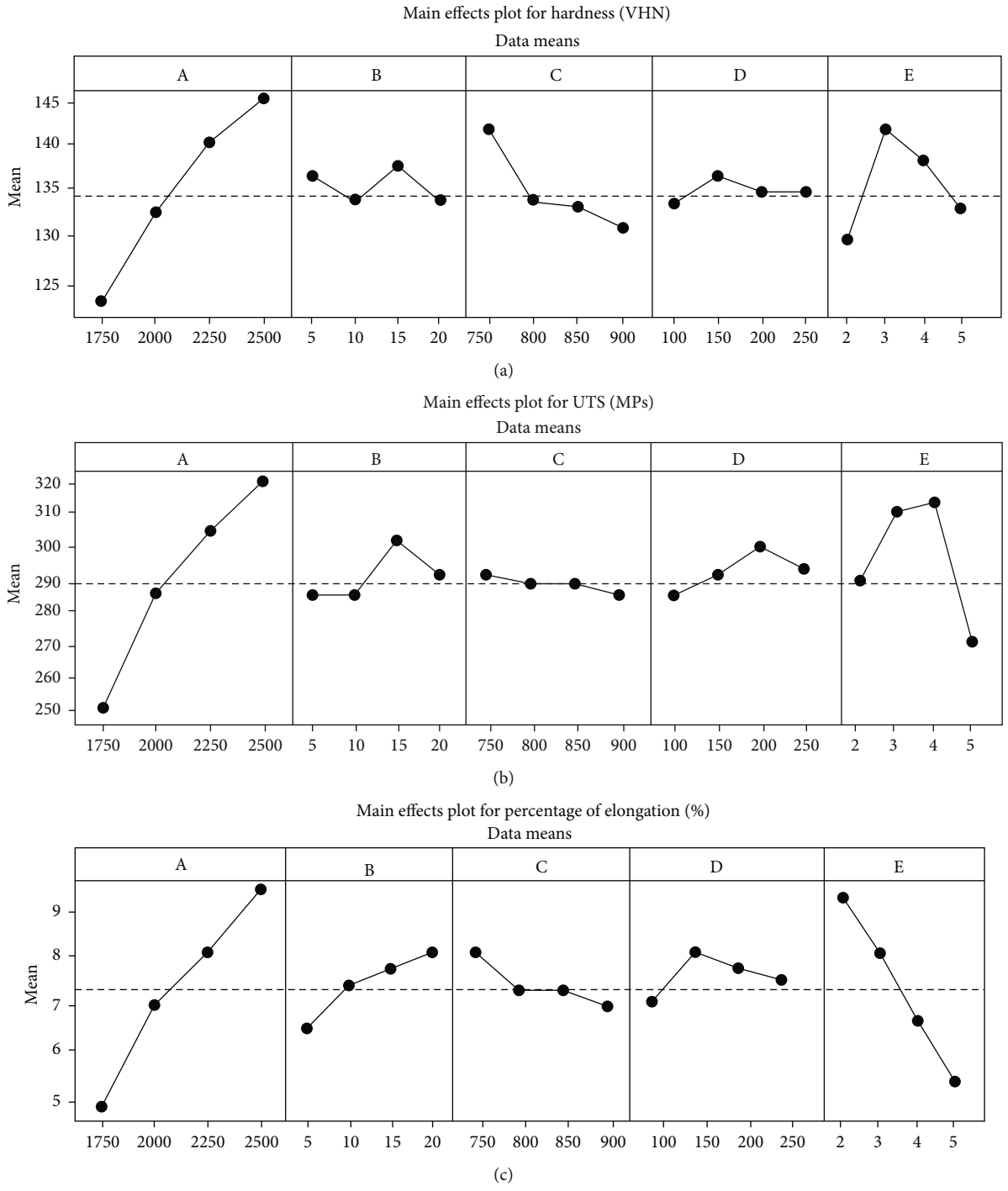

Figure 6: Continued.

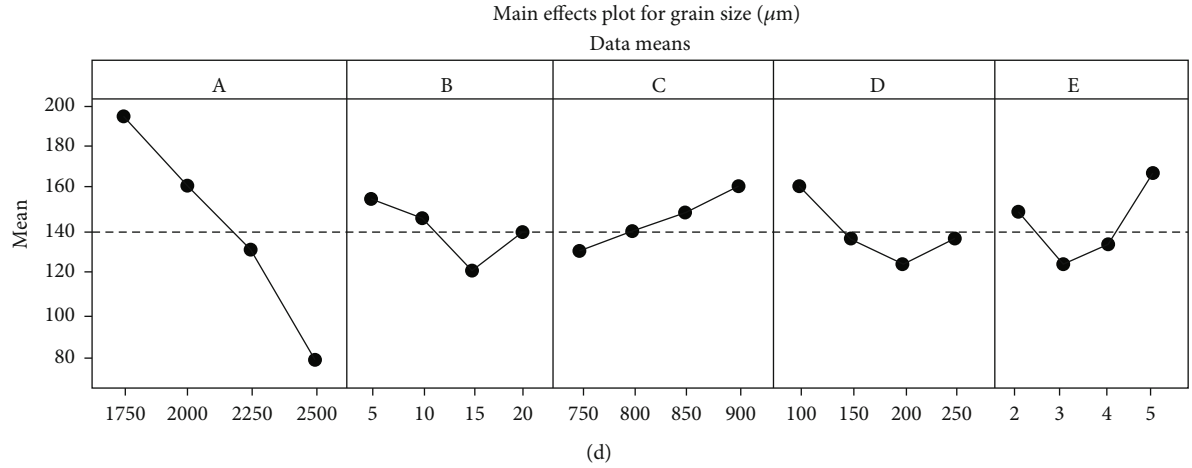

Figure 6: Main effects plots: (a) hardness, (b) ultimate tensile strength, (c) elongational %, and (d) size of the grain.

Table 8: Results of confirmation trials.

Factor setting	Initial factor	Optimum factors from Taguchi Grey response surface methodology	
		Trial values	Enhancement in response value
Level	$A_3B_3C_1D_2E_4$	Ultrasonic therapy power = 2.25367 kW Ultrasonic therapy time = 16.28 min Pouring temperature =700.73°C Squeezing pressure = 142.63 MPa Weight % of reinforcement = 1.9	
Grey relational grade	0.6199	0.8208	0.203
Hardness (VHN)	144.75	152	7.250
Ultimate tensile strength (MPa)	298.73	339.58	40.850
% of elongation (%)	6.98	10.6	3.620
Grain size (μm)	128.56	43	85.560

3.5. Influence of Factors on the Response. By means of main effect plots, it is possible to demonstrate the influence of numerous factors on the results. Plots of the principal effects for a range of responses are shown in Figures 6(a)–6(d). On the graphs, it appears that ultrasonic therapy power (A) is the most important factor in determining the correct responses. In addition to improving hardness, ultimate tensile strength, and % of elongation, increasing the UST power also reduced grain size. Intense ultrasonication at a greater ultrasonic therapy power helped disperse the nanoparticles evenly throughout the matrix. At this moment, the nanoparticles were strapped into the intergranular regions of the previously produced grains. Due to the grain's inability to spread any more as a result of this technique, an even finer grain structure was created.

With regard to ultrasonic therapy time (B), it is clear that an increase in this value enhances the replies up to a certain point in time. The ultimate tensile strength, % elongation, and particle size all improved pointedly after a 15-minute UST time. The nanoparticles were evenly disseminated throughout the matrix because of the ultrasonication procedure. As the ultrasonic therapy time increased to 20 min, the hardness, ultimate tensile strength, and elongational percentage all dropped, but the grain size improved. Due to nanoparticle aggregation, the maximum UST duration had less of an impact on the reactions of the subjects. Because of this, it is possible that an optimal ultrasonic therapy duration at midvalues is all that is needed to distribute nanoparticles effectively.

Plots of the main impacts show how answers vary depending on the weighted percentage of reinforcement used (E). Up to 3% of nanoparticles in the solution increased the reactivity. This was possible because of the uniform dispersion of nanoparticles throughout the system. Amounts of nanoparticles in excess of 3 wt% reduced the responses. It is common for nanoparticles to agglomerate in the matrix at higher percentages of the total weight. In addition to acting as stress concentration locations, the agglomerated particles also reduced mechanical responses. As a result, increasing the weight % of reinforcement reduced ultimate tensile strength and % of elongation. Table 8 shows the confirmation trials results.

Stress and strain graphs of materials manufactured under different processing conditions are shown in Figure 7. Increased ultrasonic therapy power was clearly associated with an increase in strain rate. Using high-powered sonication, a uniform dispersion of nanoparticles and fine grain refinement is achieved. Increases in nanoparticle weight % diminish elongation at various ultrasonic therapy powers, according to stress-strain curves. For example, at increased ultrasonic

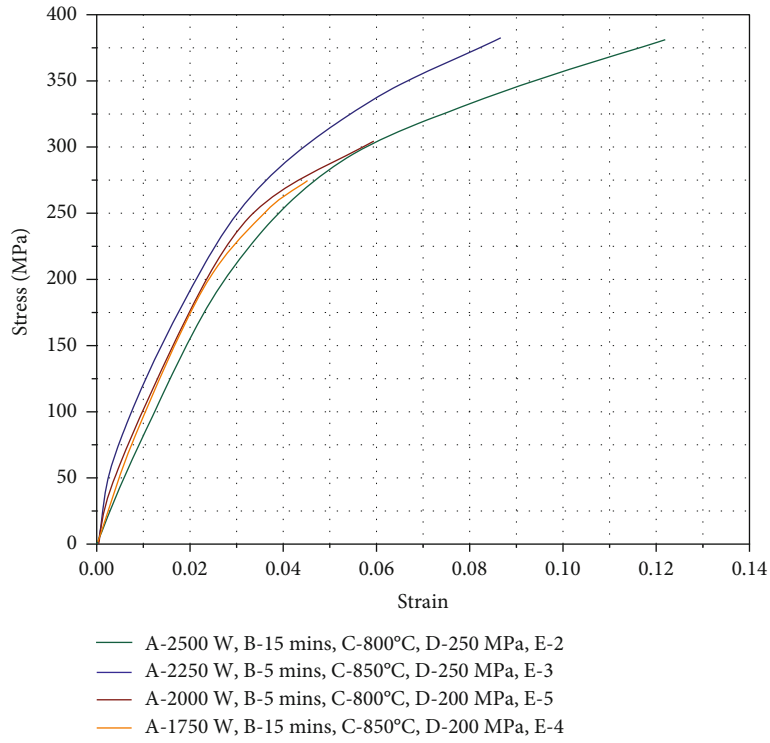

Figure 7: Tensile stress-strain curve.

therapy power, the grain fineness was greater and the dispersion of nanoparticles was more homogenous at 1.5 and 6 wt%. Consequently, the ductility improved greatly. In contrast, low-power sonication was unable to achieve uniform dispersion at high levels of reinforcement. To compensate for the loss of ductility, the material was coated with nanoparticles.

4. Conclusion

TGRSM was utilized to optimize ultrasonic therapy power, duration, pouring temperature, and the stir pressure. The investigation's findings are as follows.

(i) This study demonstrated that grain refinement, homogeneous dispersion, and nanoparticle clustering were all impacted by distinct processing factors. Zirconia particles were shown to be nonreactive with AA6061 according to XRD measurements

(ii) Multiobjective problems were transformed into similar single-objective problems using GRA. Using a model with a coefficient of determination of 0.9886, we were able to accurately predict the experimental response values. In the sixteenth trial, $A_4B_4C_1D_3E_2$ produced the greatest GRG value

(iii) As a result of these and other factors, the final results were significantly affected by the UST power and time as well as the temperature, stir pressure, and the weight percentage of reinforcement. It was found that AC, BC, and DE had significant ANOVA interactions

(iv) Response surface plots were used to describe the impacts of factors on grey relational grade, and the role of specific parameters was explored. Grain size dropped as UST power rose, yet hardness, ultimate tensile strength, and elongation % increased. Higher pouring temperatures resulted in a decreased solidification cooling rate, which resulted in better composite manufacturing outputs. At a stir pressure of 142 MPa, better responses were obtained and additional increases in pressure had very minimal effects on responses

(v) Using the TGRSM method, the following was found to be the best set of parameters: pouring temperature was 700.73°C, stir pressure was 142.63, and reinforcement was 1.9 wt%. Hardness of 151.62 VHN, ultimate tensile strength of 346.89 MPa, elongational % of 10.82, and particle size of 48.73 micrometer were found to be the optimal response parameters. Grey relational grade improved by a factor of 0.203 in the confirmation test

Data Availability

The data used to support the findings of this study are included within the article. Further data or information is available from the corresponding author upon request.

Conflicts of Interest

The authors declare that there is no conflict of interest regarding the publication of this article.

Acknowledgments

The authors extend their appreciation to the Research Center for Advanced Materials Science, King Khalid University, Saudi Arabia, for funding this work under grant number KKU/RCAMS/G011-21. Taif University Researchers Supporting Project number (TURSP-2020/01), Taif University, Taif, Saudi Arabia.

References

[1] E. M. Parsons and S. Z. Shaik, "Additive manufacturing of aluminum metal matrix composites: mechanical alloying of composite powders and single track consolidation with laser powder bed fusion," *Additive Manufacturing*, vol. 50, p. 102450, 2022.

[2] S. Banerjee, S. Poria, G. Sutradhar, and P. Sahoo, "Nanoindentation and corrosion characteristics of ultrasonic vibration assisted stir-cast AZ31–WC–graphite nano-composites," *International Journal of Metalcasting*, vol. 15, no. 3, pp. 1058–1072, 2021.

[3] S. Kolappan, T. Arunkumar, V. Mohanavel et al., "Experimental investigation on stir casted hybrid composite AA7068 with SiC and coconut shell fly ash," *Materials Today: Proceedings*, vol. 62, Part 8, pp. 5540–5545, 2022.

[4] A. Khandelwal, K. Mani, N. Srivastava, R. Gupta, and G. P. Chaudhari, "Mechanical behavior of AZ31/Al2O3 magnesium alloy nanocomposites prepared using ultrasound assisted stir casting," *Composites. Part B, Engineering*, vol. 123, pp. 64–73, 2017.

[5] J. Huang, W. Li, Y. He et al., "Temperature dependent ultimate tensile strength model for short fiber reinforced metal matrix composites," *Composite Structures*, vol. 267, p. 113890, 2021.

[6] H. Choi, W. Cho, and X. C. Li, "Semi-solid mixing for fabrication of A206/Al 2 O 3 master nanocomposites," *AFS Transactions*, vol. 121, pp. 159–164, 2013.

[7] Y. Sun, H. Choi, and X. C. Li, "Composition optimization for A206/Al2O3 nanocomposite," *AFS Transactions*, vol. 121, pp. 205–215, 2013.

[8] S.-B. Bin, S.-M. Xing, L.-M. Tian, N. Zhao, and L. Li, "Influence of technical parameters on strength and ductility of AlSi9Cu3 alloys in squeeze casting," *Transactions of Nonferrous Metals Society of China*, vol. 23, no. 4, pp. 977–982, 2013.

[9] P. Loganathan, A. Gnanavelbabu, and K. Rajkumar, "Influence of ZrB2/hBN particles on the wear behaviour of AA7075 composites fabricated through stir followed by squeeze cast technique," *Proceedings of the Institution of Mechanical Engineers, Part J: Journal of Engineering Tribology*, vol. 235, no. 1, pp. 149–160, 2021.

[10] R. Ahmad, D. T. Gethin, and R. W. Lewis, "Design element concept of squeeze casting process," *Applied Mathematical Modelling*, vol. 36, no. 10, pp. 4760–4788, 2012.

[11] T. Lu, W. Chen, B. Li et al., "Influence mechanisms of Zr and Fe particle additions on the microstructure and mechanical behavior of squeeze-cast 7075Al hybrid composites," *Journal of Alloys and Compounds*, vol. 798, pp. 587–596, 2019.

[12] S. Suresh Kumar and V. Mohanavel, "An overview assessment on magnesium metal matrix composites," *Materials Today: Proceedings*, vol. 59, pp. 1357–1361, 2022.

[13] D. Yuan, X. Yang, S. Wu, S. Lü, and K. Hu, "Development of high strength and toughness nano-SiCp/A356 composites with ultrasonic vibration and squeeze casting," *Journal of Materials Processing Technology*, vol. 269, pp. 1–9, 2019.

[14] A. H. Idrisi and A.-H. I. Mourad, "Conventional stir casting versus ultrasonic assisted stir casting process: mechanical and physical characteristics of AMCs," *Journal of Alloys and Compounds*, vol. 805, pp. 502–508, 2019.

[15] C. Allen and Q. Han, "Grain refinement of pure aluminum using ultrasonics," *International Journal of Metalcasting*, vol. 5, no. 1, pp. 69-70, 2011.

[16] X. Liu, S. Jia, and L. Nastac, "Ultrasonic cavitation-assisted molten metal processing of cast a356-nanocomposites," *International Journal of Metalcasting*, vol. 8, no. 3, pp. 51–58, 2014.

[17] A. Gnanavelbabu, K. T. S. Surendran, P. Loganathan, and E. Vinothkumar, "Effect of ageing temperature on the corrosion behaviour of UHTC particulates reinforced magnesium composites fabricated through ultrasonic assisted squeeze casting process," *Journal of Alloys and Compounds*, vol. 856, p. 158173, 2021.

[18] D. Gao, Z. Li, Q. Han, and Q. Zhai, "Effect of ultrasonic power on microstructure and mechanical properties of AZ91 alloy," *Materials Science and Engineering A*, vol. 502, no. 1–2, pp. 2–5, 2009.

[19] S. H. Mousavi Anijdan and M. Sabzi, "The effect of pouring temperature and surface angle of vortex casting on microstructural changes and mechanical properties of 7050Al-3 wt% SiC composite," *Materials Science and Engineering A*, vol. 737, pp. 230–235, 2018.

[20] B. M. Pasha and K. Mohamed, "Taguchi approach to influence of processing parameters onerosive wear behaviour of Al7034-T6 composites," *Transactions of Nonferrous Metals Society of China*, vol. 27, no. 10, pp. 2163–2171, 2017.

[21] W. Khalifa, Y. Tsunekawa, and M. Okumiya, "Ultrasonic grain refining effects in A356 Al-Si cast alloy," *AFS Transactions*, vol. 118, pp. 91–98, 2010.

[22] G. Chen, M. Yang, Y. Jin et al., "Ultrasonic assisted squeeze casting of a wrought aluminum alloy," *Journal of Materials Processing Technology*, vol. 266, pp. 19–25, 2019.

[23] G. Talla, D. K. Sahoo, S. Gangopadhyay, and C. K. Biswas, "Modeling and multi-objective optimization of powder mixed electric discharge machining process of aluminum/alumina metal matrix composite," *Engineering Science and Technology, an International Journal*, vol. 18, no. 3, pp. 369–373, 2015.

[24] P. Vijian and V. P. Arunachalam, "Optimization of squeeze casting process parameters using Taguchi analysis," *International Journal of Advanced Manufacturing Technology*, vol. 33, no. 11–12, pp. 1122–1127, 2007.

[25] X. Li, Y. Yang, and D. Weiss, "Ultrasonic cavitation based dispersion of nanoparticles in aluminum melts for solidification processing of bulk aluminum matrix nanocomposite: theoretical study, fabrication and characterization," *AFS Transactions*, vol. 2, pp. 1–12, 2007.

[26] P. C. Lynch, R. C. Voigt, J. C. Furness Jr., and D. Paulsen, "The effects of non-contact acoustic stimulation on the solidification behavior and microstructure of aluminum alloy A356," *AFS Transactions*, vol. 118, pp. 57–68, 2010.

[27] S. Wetzel, "Nano's frontier-if you think tiny particles making metals super strong sounds like sci-fi, think again," *Modern Casting*, vol. 100, p. 27, 2010.

[28] X. Jian, C. Xu, T. Meek, and Q. Han, "Effect of ultrasonic vibration on the solidification structure of A356 alloy," *AFS Transactions*, vol. 113, pp. 131–138, 2005.

[29] N. Srivastava, G. P. Chaudhari, and M. Qian, "Grain refinement of binary Al-Si, Al-Cu and Al-Ni alloys by ultrasonication," *Journal of Materials Processing Technology*, vol. 249, pp. 367–378, 2017.

[30] U. Aybarc, H. Yavuz, D. Dispinar, and M. O. Seydibeyoglu, "The use of stirring methods for the production of SiC-reinforced aluminum matrix composite and validation via simulation studies," *International Journal of Metalcasting*, vol. 13, no. 1, pp. 190–200, 2019.

[31] M. H. Sarfraz, M. Jahanzaib, W. Ahmed, and S. Hussain, "Multi-response parametric optimization of squeeze casting process for fabricating Al 6061-SiC composite," *International Journal of Advanced Manufacturing Technology*, vol. 102, no. 1–4, pp. 759–773, 2019.

[32] R. Soundararajan, A. Ramesh, N. Mohanraj, and N. Parthasarathi, "An investigation of material removal rate and surface roughness of squeeze casted A413 alloy on WEDM by multi response optimization using RSM," *Journal of Alloys and Compounds*, vol. 685, pp. 533–545, 2016.

[33] P. Madhukar, N. Selvaraj, C. S. P. Rao, and G. B. Veeresh Kumar, "Tribological behavior of ultrasonic assisted double stir casted novel nano-composite material (AA7150-hBN) using Taguchi technique," *Composites Part B: Engineering*, vol. 175, p. 107136, 2019.

[34] P. Senthil and K. S. Amirthagadeswaran, "Optimization of squeeze casting parameters for non symmetrical AC2A aluminium alloy castings through Taguchi method," *Journal of Mechanical Science and Technology*, vol. 26, no. 4, pp. 1141–1147, 2012.

[35] N. Lokesh, J. Sudheerreddy, N. G. Siddeshkumar, and K. Kotresh, "Characterization and evaluation of microstructure and mechanical properties of ZrO_2 reinforced Al6061 metal matrix composite using stir casting process," *Advances in Materials and Processing Technologies*, pp. 1–14, 2022.